HTML ABSTRACT + LINKS

Multiple-exposure holographic lithography with phase shift

Jun Hyuk Moon and Seung-Man Yang[a)]
Department of Chemical and Biomolecular Engineering, Korea Advanced Institute of Science and Technology, 373-1 Guseong-dong, Yuseong-gu, Daejeon, Korea

David J. Pine
Department of Chemical Engineering, University of California, Santa Barbara, Santa Barbara, California 93106

Won-Seok Chang
Korea Institute of Machinery and Materials, 171 Jang-dong, Yuseong-gu, Daejeon, Korea

(Received 23 June 2004; accepted 17 September 2004)

We demonstrated a multiple-exposure holographic lithography with phase shift. The phase shift was utilized to translate two-dimensional (2D) and three-dimensional (3D) interference patterns. The multiple exposure of the interference patterns with a controlled phase shift created partially overlapped patterns, resulting in 2D and 3D polymer lattices of shape-anisotropic atoms. This approach can be used to design directly the unit atoms in periodic patterns for tunable optical properties. © *2004 American Institute of Physics*. [DOI: 10.1063/1.1813644]

Lithographic pattern fabrication has been conducted by a number of methods using a patterned mask,[1] holographic interference,[2] and soft materials including self-assembled nanospheres.[3] In conventional photolithographic patterning, a polymeric substrate such as a photoresist is carved into periodic microstructures, which are used as templates for novel materials. Among the aforementioned fabrication methods, holographic lithography uses the interference pattern of multiple coherent laser beams instead of a mask in conventional photolithography processes. Simple grating patterns, two-dimensional (2D) dot arrays and three-dimensional (3D) lattice patterns can be fabricated using two-, three-, and four-beam interference, respectively. Moreover, holographic lithography has a number of desirable advantages, including one-step, large area recording, and defect-free processing.

Recently, the design of unit atoms in periodic structures has become an important issue because periodically structured materials can be used in surface relief gratings,[4] microlens arrays,[5] photonic crystal waveguides,[6] and biosensors.[7] In particular, submicron periodic structures of shape-anisotropic atoms rather than spherical isotropic atoms can modify the resonance with a light such as photonic band gaps[8,9] and dichroic optical properties.[10] In a holographic interference pattern, highly versatile patterns in 2D and 3D crystallographic groups are accessible by controlling beam properties, such as amplitude, phase, wave vector, and polarization.[11–13] In this study, we employed holographic lithography to create 2D and 3D polymer patterns that are manipulated by phase shift of laser beams. Several researchers have noted the use of an interference pattern with phase shifts for designing 2D patterns as well as 3D space groups.[14,15] Here, phase shift was utilized for the translation of the interference lattice pattern with shape-isotropic atoms. Then, multiple exposures with the phase shift created the patterns where the atoms partially overlap each other. In this way, we created 3D as well as 2D polymer patterns consisting of shape-anisotropic atoms.

Holographic lithography is based on an optical interference mask. The intensity distribution of the interference field of n coherent laser beams can be described by a Fourier superposition as

$$I = \sum_i \mathbf{E}_i^2 + \sum_{i<j} \mathbf{E}_i \cdot \mathbf{E}_j \cos[(\mathbf{k}_i - \mathbf{k}_j) \cdot \mathbf{r} + (\varphi_i - \varphi_j)], \quad i,j = 1 - n \tag{1}$$

in which $\mathbf{E}_i$, $\mathbf{k}_i$, and φ_i denote the amplitude, wave vector, and phase of beam i, respectively. The period p of the maximum (or minimum) intensity in space is inversely proportional to the difference of the wave vector, $(\mathbf{k}_i - \mathbf{k}_j)$. It is noteworthy that the phase shift that is manipulating the relative phase difference $(\varphi_i - \varphi_j)$ induces a translation of the interference pattern. Figure 1 shows the translation of the interference pattern for two linearly polarized beams. In the present study, the phase shift can be achieved by using birefringent crystals (so-called wave plates). Initially, a beam is incident on a quarter-wave plate (QWP) or a half-wave plate

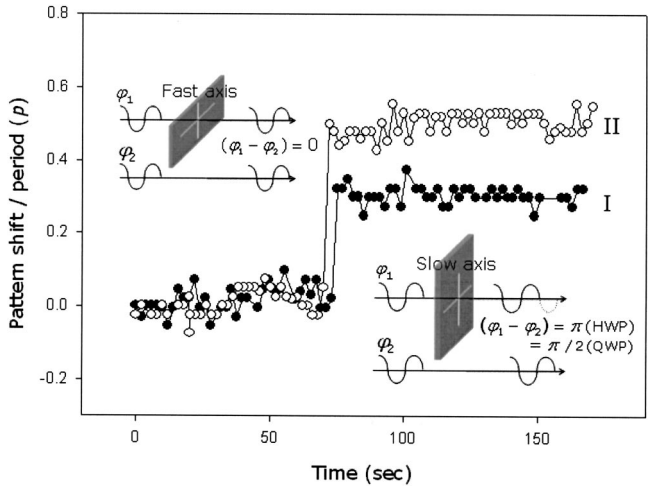

FIG. 1. The positions of the maxima of the fringe intensity as a function of time during the rotation of waveplates: (I) phase shift with a quarter-wave plate; (II) phase shift with a half-wave plate.

a)Electronic mail: smyang@kaist.ac.kr

 © 2004 American Institute of Physics
Downloaded 03 Jan 2005 to 128.111.82.73. Redistribution subject to AIP license or copyright, see http://apl.aip.org/apl/copyright.jsp

(HWP), which is linearly polarized in the direction parallel to the fast axis of the wave plate. Then, the rotation of the wave plate in such a way that the slow axis of the wave plate is parallel to the polarization direction changes the relative phase difference by $\pi/2$ for QWP and π for HWP. The phase shift with a QWP or a HWP induces the translation of the interference pattern by $p/4$ or $p/2$, respectively. Meanwhile, the position of the interference pattern was sustained within $\pm 0.06p$ for at least 1 min before and after the phase shift. For multiple exposure with a proper phase shift, wave plates were introduced after the first exposure, and the second exposure was conducted within around 1 min in order to achieve the interference stability.

In experiments, we transferred the multibeam interference pattern onto a negative photoresist, prepared using SU-8 (Shell Chemicals, Epon SU-8, glycidyl-ether-bisphenol-*A*-novolac), a photoinitator (UCB, Uvacure 1600, octoxyphenylphenyl-iodonium hexafluoro antimonate), and a photosensitizer (Spectra Group Ltd, H-Nu 470, 5,7-diiodo-3-butoxy-6-fluorene), dissolved in *r*-butyrolactone (Aldrich). We controlled the photosensitizer concentration for pattern contrast and found that the optimum weight ratio was 0.5:2.5:100. The photoresist was spin-coated on a fused silica plate. After prebaking at 65 °C, the resulting film thickness was in the range of 5–10 μm. The photoresist film was exposed to focused interfering beams. The multilaser beams were generated by splitting an Ar-ion laser (Coherent, Innova 300, 514 nm) with beam-splitters. Single-frequency operation was achieved by adding etalon to enhance the stability of the interference pattern. The dose of each exposure was 0.13–0.25 J/cm^2 and the exposed region was about 5 mm in diameter. After postexposure baking at 65 °C, the exposed film was developed in 1-methoxy-2-propanol acetate (Aldrich).

First, we considered the basic geometry in 2D structure. The interference pattern of a square lattice was created using three beams of equal intensity[16] and the intensity distribution can be written as

$$I = \sum_i^3 |\mathbf{E}_i|^2 + \mathbf{E}_1 \cdot \mathbf{E}_2 \cos[2\pi x/p + (\varphi_1 - \varphi_2)] + \mathbf{E}_2 \cdot \mathbf{E}_3 \cos[2\pi y/p + (\varphi_2 - \varphi_3)]. \quad (2)$$

The interference pattern with intensity greater than a threshold value (60% of the maximum intensity) is shown in the inset of Fig. 2(a). With this pattern, the 2D square lattice photoresist patterns were produced after a single exposure and subsequent development [Fig. 2(a)]. As noted previously, the manipulation of the relative phase difference moves the interference patterns. Here, the phase shift was achieved by rotating one QWP (i.e., from the fast axis to the slow axis of the plate or vice versa). Specifically, the phase shift of beam 1 with the QWP changes the relative phase difference $|\varphi_1 - \varphi_2|$ from the initial value by $\pi/2$ and shifts the interference pattern to the x direction by $p/4$ according to Eq. (2) [the inset of Fig. 2(b)]. Meanwhile, the phase shift of beam 3 changes the relative phase difference $|\varphi_1 - \varphi_3|$ and shifts the interference pattern to the y direction by $p/4$. [the inset of Fig. 2(c)]. Therefore, if the photoresist is exposed twice with the phase shifted second exposure, a 2D square lattice of half-overlapped atoms can be created. Figures 2(b) and 2(c) shows the SEM images of the double-exposed photoresist patterns after development. The overall patterns exhibited the

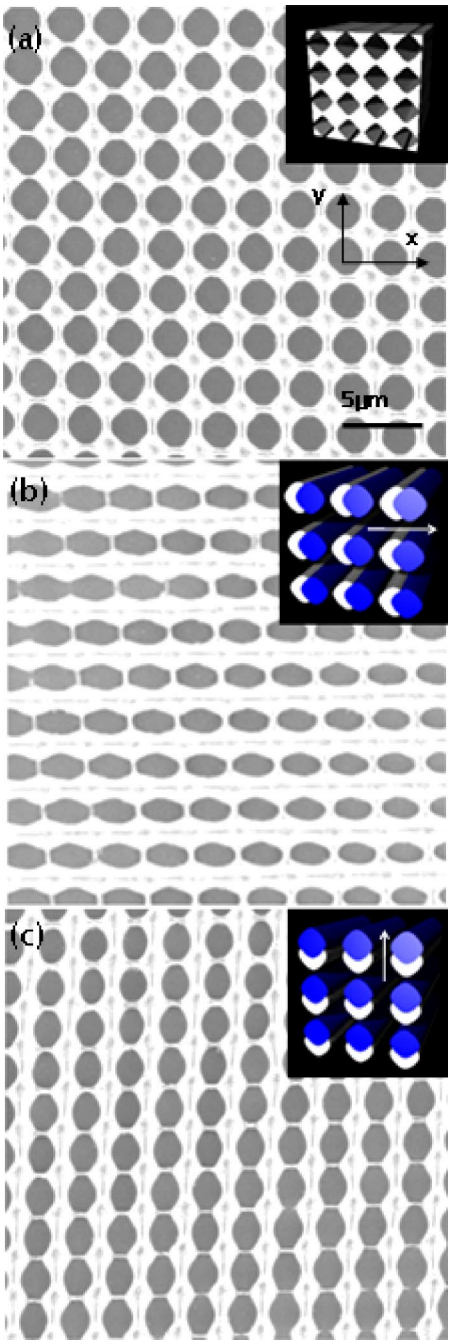

FIG. 2. (Color online) (a) SEM images of the 2D square photoresist patterns with single exposure. Inset shows the calculated interference patterns of the 2D square lattice. (b), (c) SEM images of double exposed patterns with phase shift using QWP. Insets show the first and second interference patterns in white and blue, respectively. The arrows indicate the direction of translation.

2D arrays of shape-anisotropic atoms, elongated in the x and y direction, respectively.

In the case of 3D interference patterns, a four-laser beam was assembled in an umbrella-like configuration for a fcc structure.[2] The intensity distribution of the interference pattern can be approximated by

$$I \sim \sum_i^4 |\mathbf{E}_i|^2 + \mathbf{E}_1 \cdot \mathbf{E}_2 \cos[2\pi(x - y - z)/p + (\varphi_1 - \varphi_2)] + \mathbf{E}_1 \cdot \mathbf{E}_3 \cos[2\pi(-x + y - z)/p + (\varphi_1 - \varphi_3)] + \mathbf{E}_1 \cdot \mathbf{E}_4 \cos[2\pi(-x - y + z)/p - (\varphi_1 - \varphi_4)]. \quad (3)$$

Downloaded 03 Jan 2005 to 128.111.82.73. Redistribution subject to AIP license or copyright, see http://apl.aip.org/apl/copyright.jsp

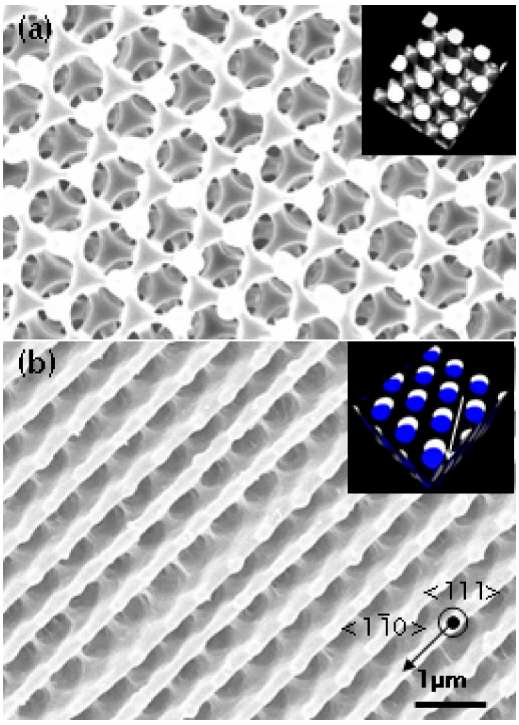

FIG. 3. (Color online) (a) SEM image of fcc photoresist patterns by single exposure. Inset is the calculated interference patterns. (b) SEM image of double exposured patterns with phase shift using two QWPs. Inset shows the locations of the first and second interference patterns in white and blue, respectively. The arrow indicates the direction of translation.

In Fig. 3(a), the transferred interference pattern shows the fcc lattice structure with a facing (111) plane, where the unit atoms are interconnected with triangular plane. (Specifically, the transferred interference pattern is an asymmetric fcc with the basis elongated in the [111] direction.[17]) In Eq. (3), the manipulation of the phase of each beam can translate the fcc interference pattern in specific direction and extent. Here, we translated the 3D interference pattern on the surface plane, that is, $[1\bar{1}0]$ direction by $p/4$. In this case, two QWPs were used to modulate two linearly polarized beams in a four-beam configuration. The phase shift was achieved by a rotation from the fast axis to the slow axis for the first beam and the other way around for the second beam. Therefore, in the second exposure, the relative phase differences, $(\varphi_1 - \varphi_2)$ and $(\varphi_1 - \varphi_3)$ in Eq. (3) were $\pi/2$ and $-\pi/2$, respectively. The inset of Fig. 3(b) displays the translation of the interference pattern. Figure 3(b) shows the surface of double-exposed photoresist pattern, where the unit atoms and interconnected plane along the $[1\bar{1}0]$ direction remain thick.

In summary, it was demonstrated that the translation of the multibeam interference pattern could be achieved by phase shift. By using a double exposure with the phase shift, 2D and 3D polymeric periodic patterns with atoms stretched along a specific direction were created successfully. This method is practically simple and direct approach for the design of unit atoms with anisotropic shape in periodic patterns. Furthermore, these polymeric patterns can be used as templates for tunable optical materials.

This work was supported by the "National R&D Project for Nano Science and Technology" of the Ministry of Science and Technology, Center for Nanoscale Mechatronics (M102KN010001-02K1401-00212), BK21 program, and CUPS-ERC. D.J.P. acknowledges support from the U.S. National Science Foundation (Grant No. CTS-0221809).

[1] M. Francois, J. Danglot, B. Grimbert, P. Mounaix, M. Muller, O. Vanbesien, and D. Lippens, Microelectron. Eng. **61**, 537 (2002).
[2] M. Campbell, D. N. Sharp, M. T. Harrison, R. G. Denning, and A. J. Turberfield, Nature (London) **404**, 53 (2000).
[3] C.-W. Kuo, J.-Y. Shiu, Y.-H. Cho, and P. Chen, Adv. Mater. (Weinheim, Ger.) **15**, 1065 (2003).
[4] N. Kawatsuki, T. Hasegawa, H. Ono, and T. Tamoto, Adv. Mater. (Weinheim, Ger.) **15**, 991 (2003).
[5] M. H. Wu, C. Park, and G. M. Whitesides, Langmuir **18**, 9312 (2002).
[6] L. Vogelaar, W. Nijdam, H. A. G. M. van Wolferen, R. M. de Ridder, F. B. Segerink, E. Fluck, L. Kuipers, and N. F. van Hulst, Adv. Mater. (Weinheim, Ger.) **13**, 1551 (2001).
[7] W. P. Qian, Z. Z. Gu, A. Fujishima, and O. Sato, Langmuir **18**, 4526 (2002).
[8] R. Wang, X.-H. Wang, B.-Y. Gu, and G.-Z. Yang, J. Appl. Phys. **90**, 4307 (2001).
[9] Z.-Y. Li, J. Wang, and B.-Y. Gu, J. Phys. Soc. Jpn. **67**, 3288 (1998).
[10] C. L. Haynes, and R. P. van Duyne, Nano Lett. **3**, 939 (2003).
[11] H. M. Su, Y. C. Zhong, X. Wang, X. G. Zheng, J. F. Xu, and H. Z. Wang, Phys. Rev. E **67**, 056619 (2003).
[12] D. N. Sharp, A. J. Turberfield, and R. G. Denning, Phys. Rev. B **68**, 205102 (2003).
[13] L. Z. Cai, X. L. Yang, and Y. R. Wang, Opt. Lett. **27**, 900 (2002).
[14] A. Chelnokov, S. Rowson, J.-M. Lourtioz, V. Berger, and J.-Y. Courtois, J. Opt. A, Pure Appl. Opt. **1**, L3 (1999).
[15] C. K. Ullal, M. Maldovan, M. Wohlgemuth, and E. L. Thomas, J. Opt. Soc. Am. A **20**, 948 (2003).
[16] For the square lattice pattern, the beam configuration satisfies $|\mathbf{k}_1 - \mathbf{k}_2| = |\mathbf{k}_2 - \mathbf{k}_3|$, $\mathbf{E}_1 \cdot \mathbf{E}_2 = 1$, $\mathbf{E}_1 \cdot \mathbf{E}_3 = 0$, $\mathbf{E}_2 \cdot \mathbf{E}_3 = 1$ with the angle between $(\mathbf{k}_1 - \mathbf{k}_2)$ and $(\mathbf{k}_2 - K_3)$ kept at 90°.
[17] Y. V. Miklyaev, D. C. Meisel, A. Blanco, G. von Freymann, K. Busch, W. Koch, C. Enkrich, M. Deubel, and M. Wegener, Appl. Phys. Lett. **82**, 1284 (2003).

Downloaded 03 Jan 2005 to 128.111.82.73. Redistribution subject to AIP license or copyright, see http://apl.aip.org/apl/copyright.jsp